minerals

MDPI

Article

Uraninite, Coffinite and Ningyoite from Vein-Type Uranium Deposits of the Bohemian Massif (Central European Variscan Belt)

Miloš René [1,*], Zdeněk Dolníček [2], Jiří Sejkora [2], Pavel Škácha [2,3] and Vladimír Šrein [4]

1 Institute of Rock Structure and Mechanics, Academy of Sciences of the Czech Republic, 182 09 Prague, Czech Republic
2 Department of Mineralogy and Petrology, National Museum, 193 00 Prague, Czech Republic; zdenek_dolnicek@nm.cz (Z.D.); jiri_sejkora@nm.cz (J.S.); skacha-p@muzeum-pribram.cz (P.Š.)
3 Mining Museum Příbram, 261 01 Příbram, Czech Republic
4 Czech Geological Survey, 152 00 Prague, Czech Republic; vladimir.srein@geology.cz
* Correspondence: rene@irsm.cas.cz; Tel.: +420-266-009-228

Received: 26 November 2018; Accepted: 15 February 2019; Published: 19 February 2019

Abstract: Uraninite-coffinite vein-type mineralisation with significant predominance of uraninite over coffinite occurs in the Příbram, Jáchymov and Horní Slavkov ore districts and the Potůčky, Zálesí and Předbořice uranium deposits. These uranium deposits are hosted by faults that are mostly developed in low- to high-grade metamorphic rocks of the basement of the Bohemian Massif. Textural features and the chemical composition of uraninite, coffinite and ningyoite were studied using an electron microprobe. Collomorphic uraninite was the only primary uranium mineral in all deposits studied. The uraninites contained variable and elevated concentrations of PbO (1.5 wt %–5.4 wt %), CaO (0.7 wt %–8.3 wt %), and SiO_2 (up to 10.0 wt %), whereas the contents of Th, Zr, REE and Y were usually below the detection limits of the electron microprobe. Coffinite usually forms by gradual coffinitization of uraninite in ore deposits and the concentration of CaO was lower than that in uraninites, varying from 0.6 wt % to 6.5 wt %. Coffinite from the Jáchymov ore district was partly enriched in Zr (up to 3.3 wt % ZrO_2) and Y (up to 5.5 wt % Y_2O_3), and from the Potůčky uranium deposit, was distinctly enriched in P (up to 8.8 wt % P_2O_5), occurring in association with ningyoite. The chemical composition of ningyoite was similar to that from type locality; however, ningyoite from Potůčky was distinctly enriched in REE, containing up to 22.3 wt % REE_2O_3.

Keywords: vein-type uranium deposits; uraninite; coffinite; ningyoite; Bohemian Massif; Variscides

1. Introduction

The Bohemian Massif is the easternmost segment of the European Variscan belt, which hosts a large number of uranium deposits (Figure 1) [1–3]. The estimated total historical production of uranium, as high as 350,000 tonnes [4], makes the Bohemian Massif the most important uranium ore district in Europe. More than three-quarters of the total uranium extracted in the territory of the Czech Republic (which slightly exceeds 100,000 tonnes) originated from ore deposits developed in fault structures hosted by metamorphic rocks, igneous rocks and/or folded sediments. Two principal types of these basement-hosted deposits can be distinguished. The first type is represented by deposits hosted by shear zones, usually containing low-grade uranium mineralisation disseminated in strongly hydrothermally altered and mylonitized rocks. Typical examples of the shear-zone hosted deposits of the Bohemian Massif include the Rožná and Olší deposits (total production 23,000 t U) and Zadní Chodov, Dyleň and Vítkov deposits (9800 t U). The second type includes vein-type deposits, characterized by open-space crystallization of hydrothermal minerals, often giving rise

to very high-grade ores. The most important examples of vein-type uranium mineralisation in the Bohemian Massif include Příbram (51,000 t U) and Jáchymov (Joachimsthal; 8500 t U) (Figure 1).

Modern data on the chemical composition of primary uranium minerals from Czech uranium deposits are, in general, very limited. Recently, several detailed studies were published [4–6], focussing on the nature and chemical composition of uraninite, coffinite and brannerite from shear-zone hosted uranium deposits, but published data on the chemical composition of uranium minerals from vein-type deposits are restricted to the Jáchymov and Zálesí deposits [7–9]. For ningyoite, which was reported from two Czech basement-hosted vein deposits [10], no complete modern analysis has been published.

This paper presents new electron microprobe data on the chemical composition of primary uranium minerals (uraninite, coffinite and ningyoite) from six typical vein-type uranium deposits of the Czech part of the Bohemian Massif (i.e., Příbram, Jáchymov, Potůčky, Horní Slavkov, Zálesí and Předbořice; Figure 1). Selection of sampling sites reflects various geological settings, paragenetic situations, intensities of superimposed alterations and probably various ages of Czech vein-type uranium deposits. Our analytical work covered a larger than average number of samples from the majority of deposits/districts studied in order to also characterize potential variability in chemical composition of primary uranium minerals at the deposit/district scale.

Besides mineralogists and economic geologists, this data on chemical composition and texture of well-localized uranium ores may also be of interest to specialists in nuclear forensics, a field that is still growing, particularly because there is an increasing international interest in the compositional analysis of radioactive minerals that can be used to fingerprint localities [11–16].

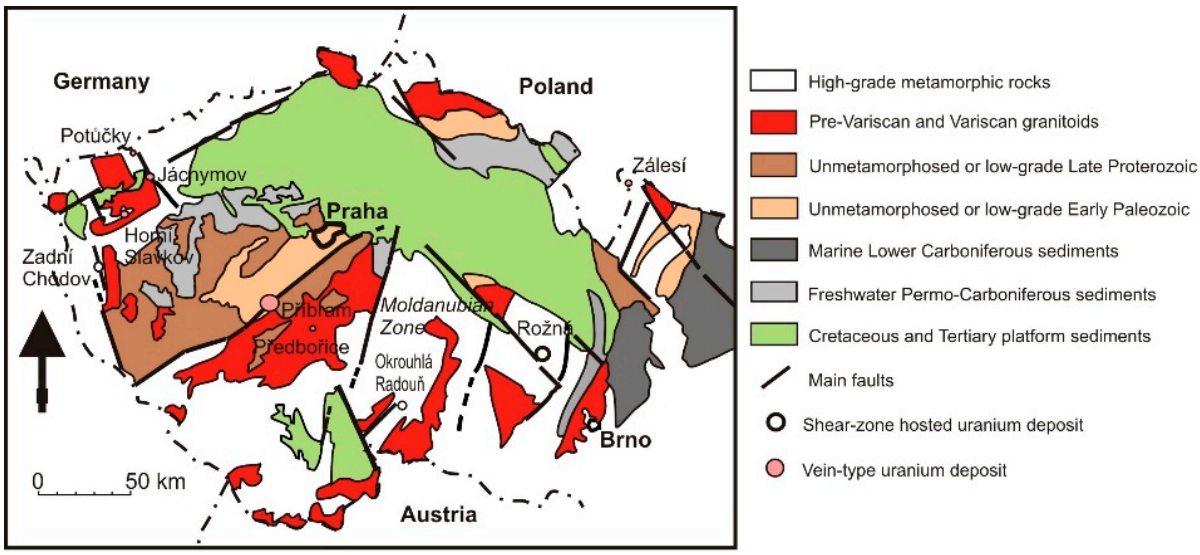

Figure 1. Simplified geological map of the Bohemian Massif showing the position of the most significant Czech basement-hosted uranium deposits.

2. Geological Setting and Mineralization

2.1. Příbram Uranium and Base Metal Districts

The Příbram uranium and base metal districts are located in the central part of the Bohemian Massif (Figure 1). This ore region consists of two main ore districts: The Březové Hory base metal district and the Příbram uranium district (Figure 2) [17], both being located in a tectonically complex zone that is situated in between the slightly metamorphosed Proterozoic-Palaeozoic of the Teplá Barrandian unit and the Variscan Central Bohemian plutonic complex (CBPC) [18]. The Březové Hory base metal district is usually subdivided into Bohutín, central Březové Hory and Černojamské ore deposits (Figure 2). The Březové Hory and Černojamské deposits were also shown to contain some uranium mineralisation (Jánská and Černojamská veins) [19,20]. The Příbram uranium district is

largely hosted by a Neoproterozoic flysch sequence (Figure 2). The ore veins form 20 vein clusters, which were grouped into nine ore knots (Třebsko, Kamenná, Lešetice, Brod, Jerusalém, Háje, Bytíz, Skalka and Obořiště; Figure 2) [21], and comprise four mineralisation stages (siderite–sulphide, calcite, calcite–uraninite and calcite–sulphide).

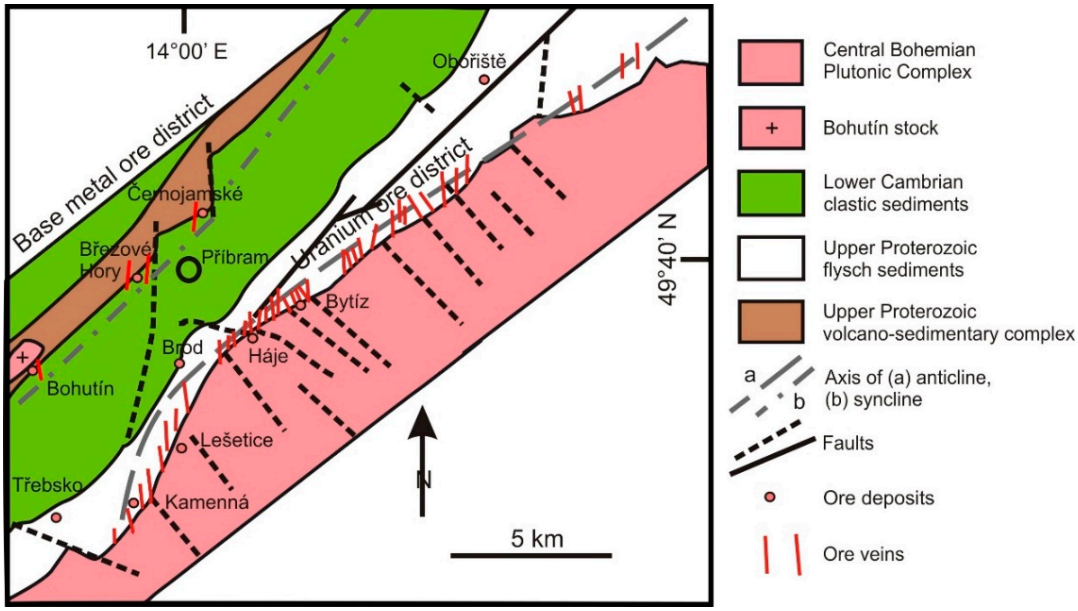

Figure 2. Schematic geological map of the Příbram base metal and uranium ore districts (modified from Kříbek et al. [17]).

The main ore minerals are uraninite and uraniferous anthraxolite, whereas coffinite is far less abundant. Bitumens from uraniferous anthraxolite were studied by Kříbek et al. [17] in greater detail. Uraninite from the Lešetice deposit was dated by Anderson [22], giving two concordant $^{206}Pb/^{238}U$ and $^{207}Pb/^{235}U$ ages (275 ± 4 Ma and 278 ± 4 Ma). The uranium minerals occur as veinlets, coatings and pods in calcite gangue. Along with this lithological control, the localization of economic mineralization was guided by structural control, displayed by the shape of individual faults, the character of the cleavage system and the position relative to the main fault and fold structures [21]. Approximately 98% of uranium ores were mined from the central part of the uranium district (Lešetice, Jerusalem, Háje and Bytíz ore segments). The whole Příbram uranium district yielded 48,432.2 t U from ores averaging 0.33 wt % U. Parallel mining of base metal and silver produced more than 6100 t of Pb, 2400 t of Zn and 28 t of Ag [2].

2.2. Jáchymov Uranium District and Potůčky Deposit

The Jáchymov uranium district covers approximately 45 km^2 of the central area of a NE–SW trending antiformal structure of the Krušné Hory/Erzgebirge Mts. This unit belongs to the Saxothuringian Zone, which is the most complex part of the central European Variscides [23]. This ore district is located at the intersection of two regional fault zones, the NW–SE striking Gera-Jáchymov fault zone and the ENE–WSW striking Krušné Hory fault zone (Figure 3) [24]. The host rocks of the Jáchymov ore district are Neoproterozoic and Cambrian metamorphic rocks of the Jáchymov series, overlying the granitic rocks of the Eibenstock-Nejdek pluton. Two vein groups could be distinguished in the Jáchymov uranium district: the ore-rich N–S veins and weakly mineralized or barren E–W veins.

Uranium mineralization is bound primarily to the carbonate-uraninite stage, but remobilised coffinite and uraninite also occur in the arsenide and sulphide stages. The published U-Pb ages cover a wide range from 76 to 286 Ma [25]. However, more precise dating from the Niederschlema-Alberoda uranium deposit, which is situated in the German part of the Jáchymov-Gera fault zone, gave ages

of 271 ± 6, 190 ± 4 and 120 ± 6 Ma for uranium minerals originating from the carbonate-uraninite, arsenic-sulphide and sulphide stages, respectively [26]. Uranium ores in the Jáchymov ore district have been mined since 1853 for the production of uranium paints and, at the beginning of the 20th century, as a source of radium. However, up to 1945, only 469.5 t U were mined [27]. From 1945 to 1994, 7950 t U were mined from ores containing an average of 0.30 wt %–0.35 wt % U. The main uranium ore production yielded the Rovnost-Eliáš-Eduard (3178.9 t U) and Eva-Barbora (1725.6 t U) ore clusters [2].

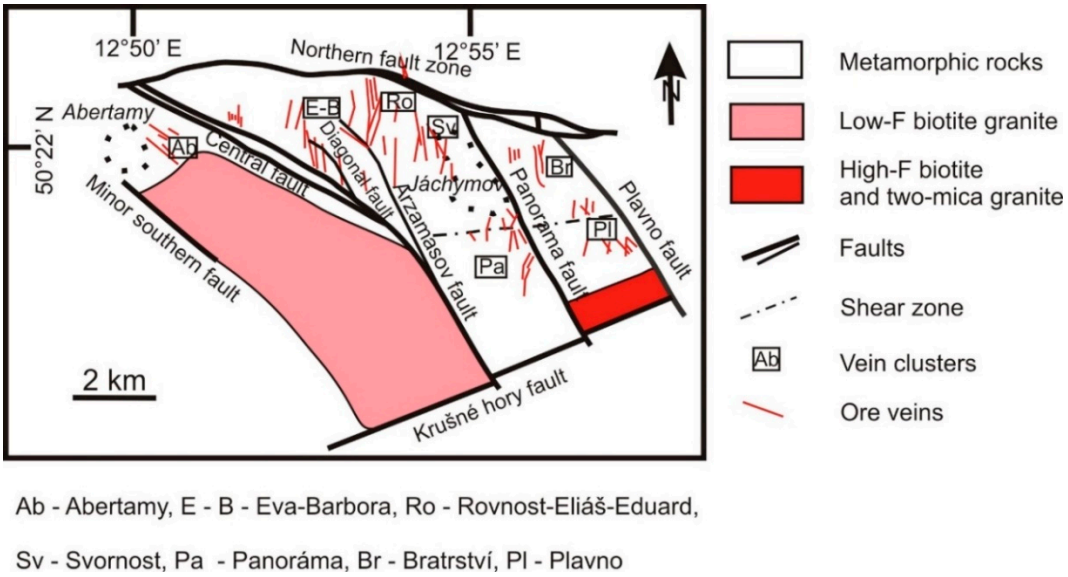

Figure 3. Schematic geological map of the Jáchymov uranium district (modified from Komínek et al. [24]).

The Potůčky deposit is a small uranium deposit situated NE of the Jáchymov ore district and on the SE edge of the Johanngeorgenstadt uranium district in Germany [28]. This uranium deposit developed in rocks of the Jáchymov series. Uranium mineralization was concentrated in NW–SE and N–S ore veins [29], whose nature is very similar to that of the Jáchymov uranium district. Uranium mineralization, represented by the calcite–uraninite stage, is formed by uraninite, coffinite and newly recognised ningyoite. Economic mineralization was concentrated at depths up to 150 m below the surface. From 1954 to 1964, the deposit yielded 323.6 t U [2,28].

2.3. Horní Slavkov Uranium District

The Horní Slavkov uranium district occurs in Proterozoic metamorphic rocks of the Slavkov crystalline unit in the western part of the Bohemian Massif (Figure 1). This unit consists of coarse-grained biotite orthogneisses and paragneiss series. The Slavkov crystalline unit was subsided below Variscan granites. Two principal fault systems—NE–SW and NW–SE—cut this crystalline unit. Uranium mineralization occurs in veins parallel to NW–SE faults and is concentrated in vein clusters (Figure 4), often being present in ore lenses and consisting of coffinite, two generations of uraninite and rarely, ningyoite [10]. The mineralization showed vertical zoning with quartz–calcite–coffinite mineralization in the upper parts of ore veins, whereas dolomite–uraninite mineralization occurred in the central parts of ore veins. The uranium mineralization mainly occurred in biotite paragneisses and amphibolites, especially at (i) the intersection of veins with faults (ii) a change in vein strike or dip and (iii) at adjoining stringers [24]. The uranium ores were mined from 1948 to 1962, yielding 2668.3 t U. The main uranium production was concentrated in the Barbora (779.3 t U), Ležnice (650.9 t U) and Zdař Bůh (539.1 t U) ore clusters [2].

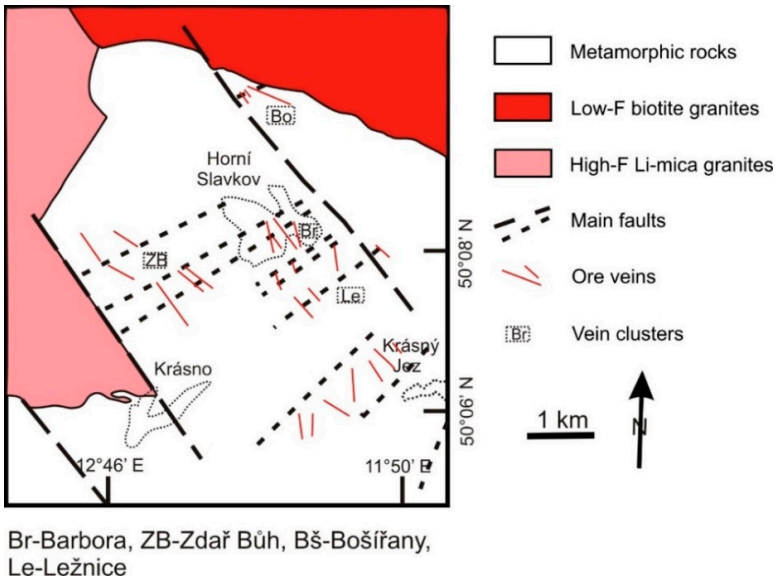

Figure 4. Schematic geological map of the Horní Slavkov uranium district (modified from Komínek et al. [24]).

2.4. Zálesí Uranium Deposit

The Zálesí uranium deposit is located on the north-eastern margin of the Bohemian Massif (Figure 1), within the Orlica-Śnieżnik crystalline complex (OSCC), an Early Palaeozoic magmatic–sedimentary sequence that was metamorphosed during the Variscan orogeny [30–32]. The OSCC is formed by metamorphic rocks of the Stronie and Śnieżnik Groups (Figure 5). The ore deposit occurs within a pocket of metamorphic rocks of the Stronie Group, which is tectonically thrust between Śnieżnik orthogneisses [32]. The rocks of the Stronie Group host all of the economic mineralization, which consists of 30 individual veins and two stockwork bodies, and mineralization was located mainly in the N–S striking complex quartz-carbonate veins up to 25 cm thick [33]. One-third of the mined ore originated from two stockwork bodies, situated within the "Central Tectonized Zone", and was composed of a dense net of subparallel veinlets. Three mineralization stages were distinguished—uraninite, arsenide and sulphide [34]. Primary uraninite was partly replaced by a coffinite-like mineral. Chemical dating by electron microprobe gave ages of 232–135 Ma (median 161 Ma), and 95–15 Ma (median 43 Ma) for uraninite and "coffinite", respectively [34]. The uranium ores of the Zálesí deposit were mined from 1959 to 1968 yielding 405.3 t U from ore containing 0.105 wt % U [2].

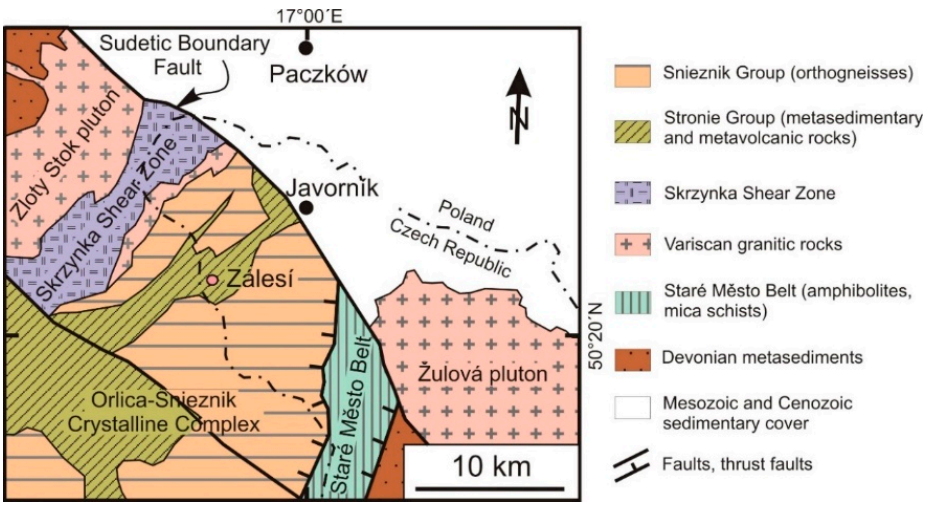

Figure 5. Geological position of the Zálesí uranium deposit (modified from Dolníček et al. [32]).

2.5. Předbořice Uranium Deposit

The Předbořice uranium deposit represents a small vein uranium deposit occurring in the Krásná Hora-Sedlčany Ordovician-Silurian metamorphic islet, in close contact with biotite granodiorites of the CBPC (Figure 1). Uranium mineralization occurs as ore lenses or veins in the N–S direction, which are predominantly hosted by the Ordovician hornfelses. The main ore mineral is uraninite and the main gangue minerals are quartz, calcite and barite. The ore mineralization contains about 20 selenides (e.g., berzelianite, bukovite, clausthalite, eskebornite, fischesserite, hakite, merenskyite, milotaite, permingeatite and petříčekite) [35–38]. Uranium ores averaging 0.39 wt % U were mined from 1965 to 1975 and the total mine production was 253.3 t U [2].

3. Material and Methods

Representative archive samples of ore mineralization from all the above deposits used for this study were collected during exploration and mining of the Czechoslovak Uranium Industry enterprise (recently DIAMO). Some samples were also collected from mine dumps at uranium ore deposits (e.g., Příbram—Bytíz, Jáchymov—Eva, Potůčky and Zálesí).

The uranium minerals were analyzed in polished sections. Back-scattered electron (BSE) images were acquired to study the internal fabric of mineral aggregates and individual mineral grains. Chemical analyses were performed using a Cameca SX-100 electron microprobe (Gennevilliers Cedex, France) (National Museum, Prague; Zdeněk Dolníček as analyst) operating in wavelength-dispersive (WDS) mode (15 kV, 10 nA and 2 μm wide beam). The following standards and X-ray lines were used to minimize line overlaps: Al—sanidine (Al K_α), As—clinoclase (As L_α), Ba—barite (Ba L_α), Bi—Bi (Bi M_α), Ca—apatite (Ca K_α), Ce—$CePO_4$ (Ce L_α), Cu—chalcopyrite (Cu K_α), Dy—$DyPO_4$ (Dy L_β), Er—$ErPO_4$ (Er L_α), Eu—$EuPO_4$ (Eu L_α), Fe—hematite (Fe K_α), Gd—$GdPO_4$ (Gd L_α), Ho—$HoPO_4$ (Ho L_β), La—$LaPO_4$ (La L_α), Lu—$LuPO_4$ (Lu M_β), Mn—rhodonite (Mn K_α), Na—albite (Na K_α), Nb—Nb (Nb L_α), Nd—$NdPO_4$ (Nd L_β), Ni—Ni (Ni K_α), P—apatite (P K_α), Pb—vanadinite (Pb M_α), Pr—$PrPO_4$ (Pr L_β), S—celestite (S K_α), Sc—$ScVO_4$ (Sc K_α), Si—wollastonite (Si K_α), Sm—$SmPO_4$ (Sm L_α), Sr—celestite (Sr L_β), Tb—$TbPO_4$ (Tb L_α), Th—Th (Th M_α), Ti—TiO_2 (Ti K_α), Tm—$TmPO_4$ (Tm L_α), U—UO_2 (U M_α), V—V (V K_α), W—scheelite (W M_α), Y—YVO_4 (Y L_α), Yb—$YbPO_4$ (Yb L_α), Zn—ZnO (Zn K_α), Zr—zircon (Zr L_α).

Peak counting times were 20 s for all elements and one-half of the peak time for each background. Contents of the elements listed, which are not included in tables, were analyzed quantitatively, but had contents below the detection limit (ca. 0.01 wt %–0.04 wt % for most elements, around 0.1 wt %–0.3 wt % for REEs). Raw intensities were converted into concentrations of elements using automated "PAP" matrix-correction software [39].

When reporting the chemical composition of primary uranium minerals, the median values for each deposit were used, as it is less sensitive to extreme values than the mean. The all performed analyses of uraninite, coffinite and ningyoite are published as Supplementary Materials (Tables S1–S3). To represent the full variation, minimum and maximum values are also reported (Tables 1–3). For selected elements, the Spearman correlation coefficients were presented (Tables 4 and 5). These were preferred over Pearson correlation coefficients, as there are more robust to aberrant values.

4. Results

The predominant uranium mineral in samples from all uranium deposits studied was uraninite. Coffinite, which was also identified in our samples, was relatively rare. Uranium-bearing anthraxolite contained grains of uraninite and occurred only in the Příbram uranium district (ore clusters Bytíz and Lešetice). Ningyoite was newly found as a very rare uranium mineral in some uraninite-rich dump samples from the Potůčky deposit.

4.1. Uraninite

Uraninite usually occurred in the form of spherical or botryoidal aggregates enclosed in carbonate gangue and/or was associated with quartz. In some cases, uraninite spheroids showed radial fractures that provided pathways for younger hydrothermal solutions. The activity of younger silica-rich solutions resulted in superimposed coffinitization of uraninite.

In the Příbram uranium district, uraninite occurred as spherical or botryoidally evolved aggregates, fine veinlets and fine bands within calcite (Figure 6A,B). Relatively rare uraninite II occurred in later calcite–sulphide stages and formed fine spherical coatings close to older uraninite from the calcite–uraninite stage (Figure 6C). Uraniferous anthraxolite formed irregular fragments, rounded grains and veinlets within calcite. Its uranium content was concentrated in numerous inclusions of uraninite (and minor coffinite), which typically showed a disintegrated/cracked nature (Figure 6D).

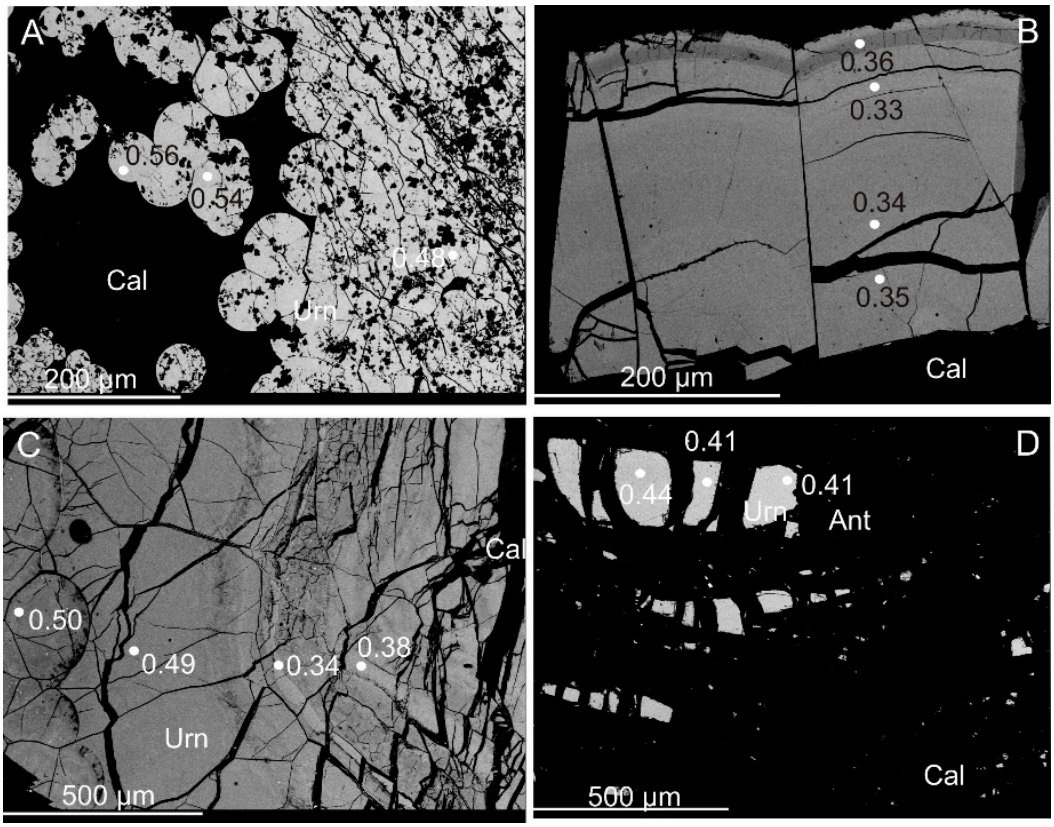

Figure 6. Back-scattered electron (BSE) images of uranium mineralization with distribution of Ca (*apfu*, O = 4) in uraninite, Příbram uranium district. (**A**) Botryoidally evolved aggregates of uraninite; (**B**) Detailed distribution of Ca in botryoidally evolved uraninite; (**C**) Detailed distribution of Ca in partly zoned uraninite; (**D**) Distribution f Ca in uraninite included in anthraxolite. Urn—uraninite, Cal—calcite, Ant—anthraxolite.

In the Jáchymov uranium district uraninite formed massive spherical aggregates or thin veinlets lining wall rocks, while the central areas of the veins were filled with dolomite pigmented by Fe-oxides (Figure 7A,B). The spherical morphology of the uraninite aggregates was likewise characteristic for Potůčky and Horní Slavkov. In the Zálesí uranium deposit, uraninite occurred in the form of spherical and/or zoned aggregates (Figure 8A,B).

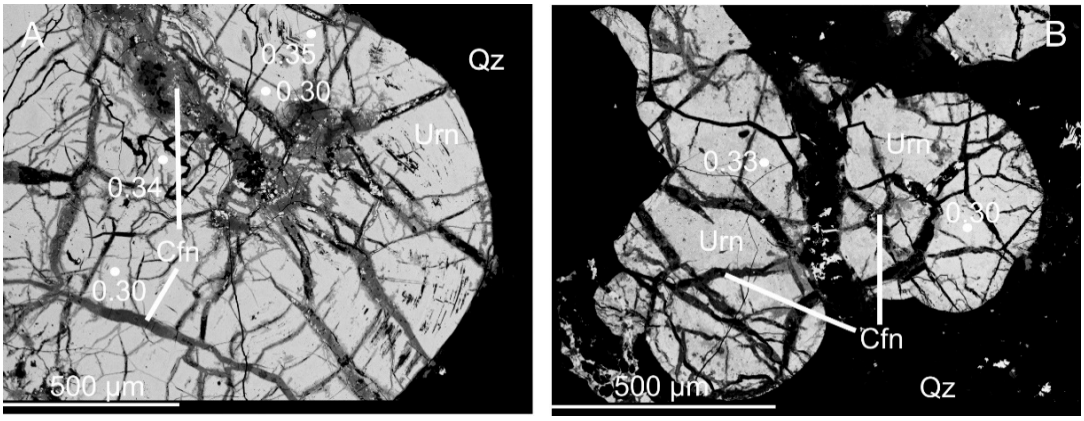

Figure 7. BSE images of uranium mineralization from the Jáchymov uranium district with distribution of Ca (*apfu*, O = 4). (**A**) Distribution of Ca in partly zoned uraninite; (**B**) Distribution of Ca in botryoidally evolved uraninite. Urn—uraninite, Cfn—coffinite, Qz—quartz.

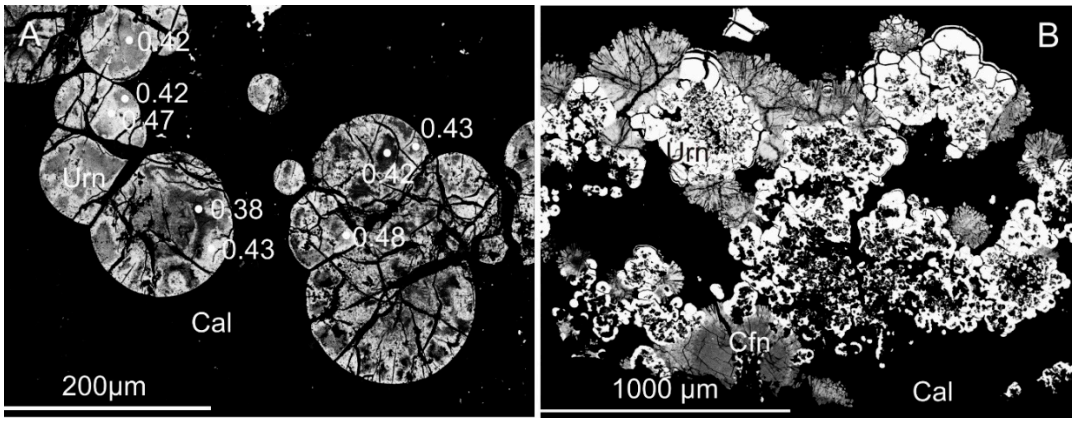

Figure 8. BSE images of uranium mineralization with distribution of Ca (*apfu*, O = 4) in uraninite, Zálesí uranium deposit. (**A**) Distribution of Ca in botryoidally evolved uraninite; (**B**) Intergrowths of uraninite with coffinite. Urn—uraninite, Cfn—coffinite, Cal—calcite.

The UO_2 content in uraninite from the vein-type ore deposits studied was quite variable, ranging from 65.40 wt % to 81.80 wt %. All other constituents varied significantly: the PbO content varied from 0.10 wt % to 10.81 wt %, SiO_2 from 0.0 wt % to 9.98 wt %, FeO from 0.0 wt % to 4.15 wt % and CaO from 0.69 wt % to 8.31 wt % (Table 1). Concentrations of P, Th and Zr were relatively low: up to 1.11 wt % P_2O_5, up to 0.12 wt % ThO_2 and up to 1.79 wt % ZrO_2. The highest concentration of PbO was found in uraninite from Příbram (up to 10.81 wt %), the highest concentration of CaO was found in uraninite from Horní Slavkov (up to 8.31 wt %) and the highest concentration of SiO_2 was found in uraninite from the Předbořice deposit (up to 9.98 wt %). The concentrations of REE in the majority of the uraninites analyzed were below the detection limits of the electron microprobe. The concentrations of Y were mostly also low; the highest concentrations were found in uraninite from Zálesí (up to 2.32 wt % Y_2O_3; Table 1).

Table 1. Ranges of selected components in the uraninites studied.

Locality	Jáchymov			Potůčky			Horní Slavkov		
	n = 81			*n* = 50			*n* = 23		
(wt %)	Min.	Max.	Median	Min.	Max.	Median	Min.	Max.	Median
UO_2	67.82	86.56	81.80	70.00	86.77	81.80	70.30	81.23	75.54
ThO_2	b.d.l.	0.08	0.00	b.d.l.	0.12	0.00	b.d.l.	0.10	0.00
PbO	0.09	10.23	1.83	b.d.l.	6.51	1.53	0.10	4.74	3.71
SiO_2	b.d.l.	9.48	1.67	b.d.l.	9.51	1.66	0.25	9.84	5.30
P_2O_5	b.d.l.	0.36	0.09	b.d.l.	1.11	0.17	b.d.l.	0.18	0.05
Al_2O_3	b.d.l.	0.73	0.06	b.d.l.	0.58	0.09	b.d.l.	1.00	0.33
ZrO_2	b.d.l.	1.79	0.00	b.d.l.	0.19	0.05	b.d.l.	0.03	0.00
CaO	0.69	7.41	4.14	0.85	6.11	2.81	1.39	8.31	4.92
FeO	0.23	4.15	0.59	0.41	3.13	0.86	b.d.l.	4.10	0.89
As_2O_5	b.d.l.	6.09	0.78	0.08	5.16	0.96	b.d.l.	2.13	0.27
Y_2O_3	b.d.l.	1.24	0.22	b.d.l.	1.62	0.89	b.d.l.	0.16	0.00
Locality	Příbram			Zálesí			Předbořice		
	n = 101			*n* = 45			*n* = 64		
(wt %)	Min.	Max.	Median	Min.	Max.	Median	Min.	Max.	Median
UO_2	69.76	88.03	81.16	65.40	84.60	74.84	70.90	88.38	81.35
ThO_2	b.d.l.	0.09	0.00	b.d.l.	0.08	0.00	b.d.l.	0.09	0.00
PbO	0.13	10.81	5.36	0.31	10.28	2.33	0.49	5.60	3.07
SiO_2	b.d.l.	6.83	0.68	0.57	9.25	2.51	b.d.l.	9.98	1.03
P_2O_5	b.d.l.	0.23	0.07	b.d.l.	0.33	0.02	b.d.l.	0.22	0.02
Al_2O_3	b.d.l.	0.48	0.05	b.d.l.	0.72	0.04	b.d.l.	0.23	0.02
ZrO_2	b.d.l.	0.14	0.00	b.d.l.	0.11	0.00	b.d.l.	0.04	0.00
CaO	1.28	6.24	4.56	1.40	5.41	3.27	2.94	7.93	5.08
FeO	b.d.l.	1.05	0.07	0.16	2.01	0.58	b.d.l.	1.04	0.03
As_2O_5	0.06	2.03	0.44	b.d.l.	4.12	0.70	b.d.l.	0.37	0.16
Y_2O_3	b.d.l.	0.26	0.00	0.04	2.32	0.62	b.d.l.	0.09	0.00

b.d.l.—below detection limit.

4.2. Coffinite

Coffinite occurs predominantly as pseudomorphs after uraninite, or in the form of coatings, irregular clusters or small grains in younger cracks hosted by spherical aggregates of uraninite. In the Příbram uranium district, coffinite occurred as irregular clusters or small grains in cracks later filled with calcite and fine younger disseminations along with larger uraninite grains (Figure 9A). Uraniferous anthraxolite, together with predominating inclusions of uraninite, sometimes contained small isometric anhedral grains of coffinite (Figure 9B). In the Jáchymov uranium district, coffinite occurred in concentric and radial fractures in uraninite spheroids as younger thin rims growing over spherical aggregates of uraninite and as pseudomorphs after uraninite spheroids (Figure 10A,B). In the Potůčky deposit, the coffinitized uraninite and coffinite were found as pseudomorphs after older uraninite spheroids and as irregular disseminations among these spheroids. In the Horní Slavkov uranium district, coffinite occurred as small grains in fractures of massive uraninite. For the Zálesí deposit, coffinitized uraninite and radial aggregates of a coffinite-like mineral growing over older

uraninite were significant (Figure 11). The coffinitized uraninite also occurred in zoned uraninite spheroids from the Předbořice deposit.

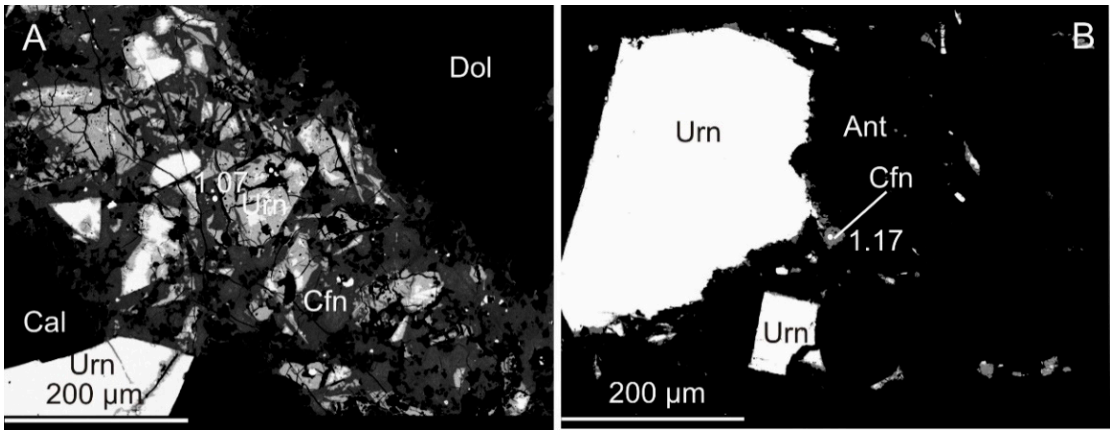

Figure 9. BSE images of uranium mineralization with distribution of Si (*apfu*, O = 4) in coffinite, Příbram uranium district. (**A**) Distribution of Si in coffinite enclosed in calcite; (**B**) Distribution of Si in coffinite that is enclosed in antraxolite. Urn—uraninite, Cfn—coffinite, Ant—anthraxolite, Cal—calcite, Dol—dolomite.

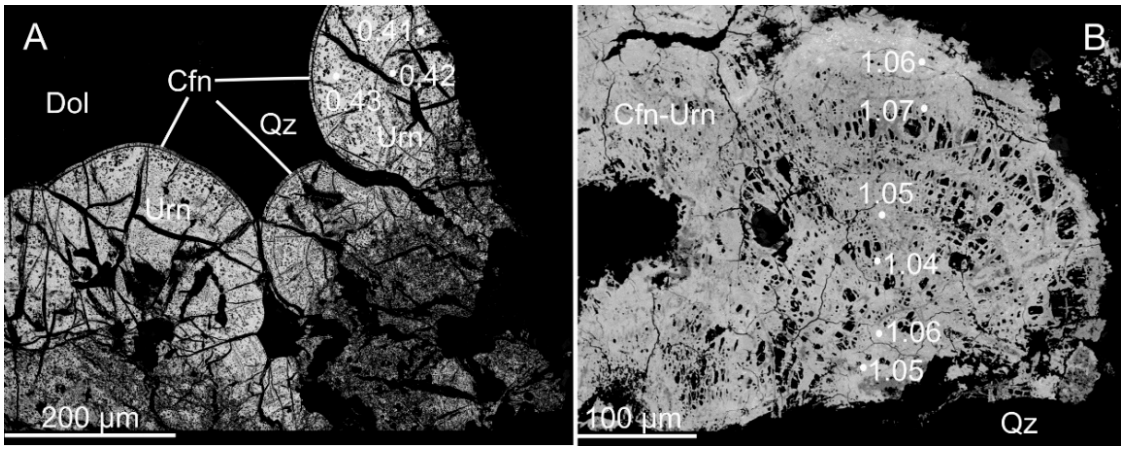

Figure 10. BSE images of coffinite and coffinitized uraninite with distribution of Si (*apfu*, O = 4), Jáchymov uranium district. (**A**) Distribution of Si in partly coffinitized uraninite; (**B**) Detailed distribution of Si in botryoidally evolved uraninite. Urn—uraninite, Cfn—coffinite, Cfn-Urn—coffinitized uraninite, Dol—dolomite, Qz—quartz.

The concentrations of UO_2 and SiO_2 in coffinite from the vein-type deposits studied were highly variable, ranging from 50.59 wt % to 74.09 wt % and from 10.1 wt % to 28.15 wt %, respectively. All other elements also varied significantly: the PbO content varied from 0.0 wt % to 7.41 wt %, FeO from 0.0 wt % to 5.25 wt %, CaO from 0.69 wt % to 6.49 wt % and P_2O_5 from 0.0 wt % to 8.79 wt % (Table 2). Anomalously high levels of P were found in coffinite from Potůčky (up to 8.79 wt % P_2O_5). Concentrations of Th and Zr in coffinite were relatively low: up to 0.21 wt % ThO_2 and up to 3.3 wt % ZrO_2. The highest concentrations of Pb and Ca were found in coffinite from the Zálesí deposit (up to 7.41 wt % and 5.67 wt % PbO and CaO, respectively). The highest concentration of Si was found in coffinite from the Horní Slavkov uranium district (up to 28.15 wt % SiO_2). The concentrations of REE were usually below detection limits. The concentrations of Y in the coffinite analyzed were mostly low. The highest concentration of Y was found in coffinite from the Zálesí deposit (up to 9.41 wt % Y_2O_3; Table 2).

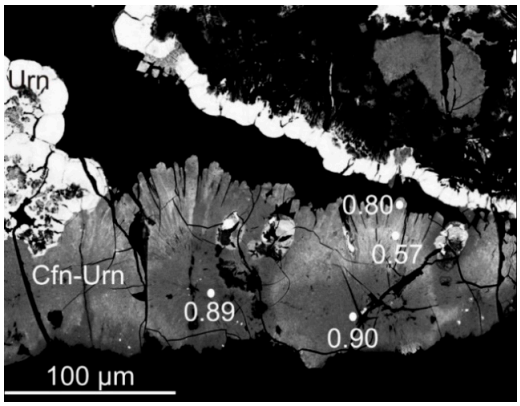

Figure 11. BSE image of coffinitized uraninite with distribution of Si (*apfu*, O = 4), Zálesí uranium deposit. Urn—uraninite, Cfn-Urn—coffinitized uraninite.

Table 2. Concentration ranges of selected components in coffinite.

Locality	Jáchymov			Potůčky			Horní Slavkov		
	n = 48			*n* = 15			*n* = 12		
(wt %)	Min.	Max.	Median	Min.	Max.	Median	Min.	Max.	Median
UO_2	50.59	74.09	62.91	57.85	65.96	63.67	53.65	75.20	64.09
ThO_2	b.d.l.	0.19	0.00	b.d.l.	0.09	0.00	b.d.l.	0.21	0.00
PbO	b.d.l.	0.12	0.00	b.d.l.	1.10	0.01	b.d.l.	4.48	0.30
SiO_2	10.47	23.43	17.63	12.67	16.68	13.52	10.23	28.15	21.67
P_2O_5	b.d.l.	5.02	0.85	0.46	8.79	7.83	0.12	0.91	0.42
Al_2O_3	0.06	2.15	0.82	0.04	1.72	0.20	0.44	2.08	1.05
ZrO_2	b.d.l.	3.30	0.02	b.d.l.	0.18	0.02	b.d.l.	0.19	0.00
CaO	0.69	4.35	2.39	0.82	4.14	3.75	1.30	3.52	1.71
FeO	0.03	3.90	0.37	0.63	5.25	0.99	0.29	2.29	1.12
As_2O_5	b.d.l.	5.25	0.39	0.88	3.98	1.16	0.13	1.96	0.03
Y_2O_3	b.d.l.	5.46	0.84	0.11	2.46	2.22	b.d.l.	0.33	0.07
Locality	Příbram			Zálesí			Předbořice		
	n = 20			*n* = 26			*n* = 2		
(wt %)	Min.	Max.	Median	Min.	Max.	Median	Min.	Max.	Mean
UO_2	52.48	69.33	65.48	52.80	71.46	65.35	69.06	72.24	70.65
ThO_2	b.d.l.	0.15	0.00	b.d.l.	0.11	0.00	b.d.l.	0.11	0.06
PbO	b.d.l.	1.74	0.56	b.d.l.	7.41	0.46	1.04	4.87	2.96
SiO_2	14.40	25.69	17.87	10.10	24.07	14.06	11.69	12.49	12.09
P_2O_5	b.d.l.	0.41	0.15	b.d.l.	4.12	0.11	0.20	0.43	0.32
Al_2O_3	0.22	2.19	0.83	b.d.l.	2.26	0.11	0.19	0.29	0.24
ZrO_2	b.d.l.	0.17	0.00	b.d.l.	0.15	0.00	b.d.l.	0.11	0.06
CaO	1.24	6.49	2.45	0.56	5.67	2.76	5.27	5.64	5.46
FeO	0.02	1.52	0.44	b.d.l.	1.95	0.16	0.45	0.87	0.66
As_2O_5	b.d.l.	0.96	0.26	b.d.l.	4.76	0.91	0.07	0.14	0.11
Y_2O_3	b.d.l.	2.06	0.37	0.15	9.41	1.13	b.d.l.	0.09	0.06

b.d.l.—below detection limit.

4.3. Ningyoite

Ningyoite was only found in samples from the Potůčky uranium deposit. It occurred as an irregular filling of fractures in older uraninite, sometimes together with coffinite (Figure 12A,B). The concentration of UO_2 in ningyoite was variable, ranging from 20.45 wt % to 35.93 wt %. All other constituents also varied significantly: the P_2O_5 content varied from 20.31 wt % to 26.07 wt %, REE_2O_3 from 13.54 wt % to 22.60 wt %, CaO from 7.5 wt % to 9.7 wt %, Y_2O_3 from 1.93 wt % to 4.46 wt %, PbO from 1.31 wt % to 6.56 wt % and FeO from 0.39 wt % to 0.97 wt % (Table 3). The concentrations of Th and Zr were usually below detection limits.

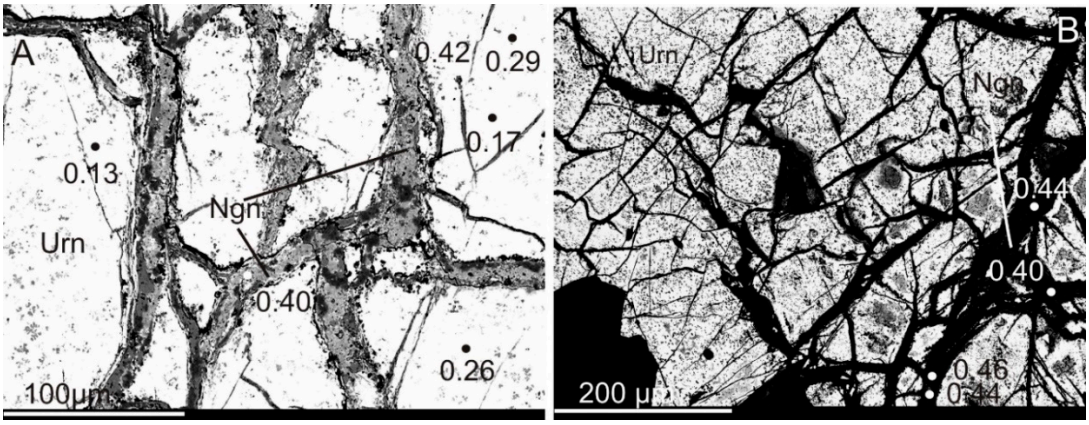

Figure 12. BSE images of uranium mineralization with distribution of Ca (*apfu*, O = 4) in ningyoite and uraninite, Potůčky uranium deposit. (**A**) Distribution of Ca in ningyoite and uraninite, (**B**) Detailed BSE image of distribution of Ca in ningyoite. Urn—uraninite, Ngn—ningyoite.

Table 3. Ranges of contents of selected components in the studied ningyoite.

Locality	**Potůčky**		
(wt %)	**Min.**	**Max.**	**Median**
UO_2	20.45	35.93	26.58
ThO_2	b.d.l.	b.d.l.	0.00
PbO	1.31	6.56	4.64
SiO_2	b.d.l.	3.03	0.59
P_2O_5	20.31	26.07	24.17
Al_2O_3	b.d.l.	0.35	0.09
ZrO_2	b.d.l.	0.30	0.00
CaO	7.50	9.74	8.67
FeO	0.39	0.97	0.63
As_2O_5	b.d.l.	0.43	0.14
Y_2O_3	1.93	4.46	3.15
REE_2O_3	13.54	22.26	16.70

b.d.l.—below detection limit.

5. Discussion

5.1. Composition of Uraninite

Uraninite, nominally UO_2, occurs in nature as a non-stoichiometric mineral with a highly defective fluorite structure. The non-stoichiometry and defects are caused by oxidation of uranium, cationic substitutions and α-decay damage. During the oxidation of U^{4+} to U^{6+} in UO_2, excess oxygen is incorporated into the structure causing the formation of non-stoichiometric UO_{2+x}, where x is the number of excess interstitial oxygens. This non-stoichiometric mineral always contains cation impurities, e.g., Pb, Ca, Th, Zr, Y and REE. Therefore, its chemical formula may be written better as

$(U^{4+}{}_{1-x-y-z-v}U^{6+}{}_{x}REE^{3+}{}_{y}M^{2+}{}_{z}\square^{4-}{}_{v})O_{2-(0.5y)-2v}$, where x is the amount of excess oxygen equal to U^{6+}, y is the number of trivalent cations (REE + Y), z is the number of divalent cations (Pb, Ca), and v is number of uranium vacancies in the unit formula [40,41]. Concentrations of these intrinsic elements may exceed 20 wt %.

Radiogenic Pb is a major impurity in uraninites of great age. Up to 21.4 wt % PbO were found in uraninites from the Proterozoic unconformity-related uranium deposits in Canada, whereas uraninites from the Variscan uranium deposits in France contained only up to 4.9 wt % PbO [42,43]. The concentrations of Pb in uraninites from the Czech vein-type deposits studied mostly ranged from 1.5 wt % to 5.4 wt % PbO. These concentrations are very similar to those in uraninites from vein-type deposits in the German part of the Krušné Hory-Erzgebirge Mts. (Schneeberg, Schlema-Alberoda)—1.5 wt %–5.5 wt % PbO [43,44]. With respect to the Variscan (i.e., Permian) age of uranium mineralization in the Bohemian Massif [22,25], the high contents of PbO, up to 10.81 wt % recorded in some uraninites from the Příbram, Zálesí and Jáchymov deposits, cannot be considered to represent radiogenic lead generated by in-situ decay of uranium. Instead, one can assume co-precipitation of common lead during crystallization of uraninite, and/or redistribution of lead during superimposed hydrothermal alteration of uraninite. The presence of growth zones rich in lead, which have been observed in samples from the Příbram uranium deposit, strongly favours the first possibility. The absence of a statistically significant correlation between the contents of Pb and U observed at all sites studied (correlation coefficients $\leq$0.48; Table 4) implies the involvement of multiple processes affecting the chemical composition of uraninite, including growth of radiogenic lead with time, co-precipitation of common lead during crystallization of uraninite and/or superimposed hydrothermal alteration associated with loss of lead.

A substitution of the type $2U^{4+} = (U^{6+} + Ca^{2+})$ has been proposed in oxidised Ca-rich uraninite [7]. Concentrations of Ca in the uraninites analyzed varied from 0.7 wt % to 8.3 wt % CaO. The highest Ca content in uraninite from the Horní Slavkov uranium district (up to 8.3 wt % CaO) together with a positive correlation between CaO and PbO (correlation coefficient 0.72; Table 4), suggests significant oxidation of uraninite (Figure 13). A similar relationship between Ca and Pb was also observed at the Zálesí deposit (correlation coefficient 0.74; Table 4), but at other sites no statistically significant correlations between both elements were found (correlation coefficients $\leq$0.41; Table 4). The concentrations of Ca in other vein-type uranium deposits (Great Bear Lake and Algoma, Canada, Armorican Massif and Massif Central, France) ranged from 1.3 wt % to 9.5 wt % CaO [42–45].

The close association of sulphides and bitumens with coffinite is evidence of reducing conditions during coffinitization [41]. With the exception of Horní Slavkov, negative correlations occurred between concentrations of CaO and SiO_2 (correlation coefficients from −0.38 to −0.84; Table 4), suggesting reducing conditions during coffinitization of uraninite. Concentrations of Si in uraninites from the Variscan uranium deposits in France also varied considerably, from 0.1 wt % to 5.1 wt % SiO_2 [42].

The concentrations of Th in uraninites from vein-type uranium deposits were usually very low, typically below detection limits of the electron microprobe [37]. In our samples, the highest concentrations of Th were found in uraninite from the Horní Slavkov district (up to 0.21 wt % ThO_2). However, the majority of our uraninite analyses displayed concentrations of ThO_2 below the detection limits. Worldwide, the highest concentrations of Th have been found in uraninites from the Precambrian Witwatersrand conglomerate-hosted uranium deposits in South Africa (up to 9.5 wt % ThO_2) and the Proterozoic unconformity-related deposits in Canada (up to 3.8 wt % ThO_2) [13,43].

The concentrations of Zr in uraninites from vein-type uranium deposits were usually also low, mostly below the detection limit [13]. However, Zr-enriched uraninite was described from a vein-type deposit in North Eastern Egypt, containing up to 2.49 wt % ZrO_2 [46]. The Zr-enriched uraninites occurred in sandstone-type uranium deposits [47]. The highest content of Zr was found in amber from the North Bohemian Cretaceous sandstone-type uranium ore district, containing up to 4.97 wt % ZrO_2 [48]. In uraninite samples from vein-type deposits of the Bohemian Massif, the Zr concentrations were also low. Enrichment of up to 0.66 wt % ZrO_2 was found only in uraninite from

the Jáchymov uranium district. A similar enrichment in Zr in uraninite from Jáchymov was also found by Frimmel et al. [13]; however, the authors interpreted such elevated contents of Zr in terms of the presence of discrete inclusions of a Zr-mineral.

Table 4. Spearman correlation coefficients for selected elements analyzed in uraninite.

Jáchymov	**UO_2**	**PbO**	**SiO_2**	**P_2O_5**	**CaO**	**Al_2O_3**	**Y_2O_3**
UO_2	1.00						
PbO	−0.01	1.00					
SiO_2	−0.72	−0.20	1.00				
P_2O_5	0.14	−0.32	0.14	1.00			
CaO	0.49	−0.05	−0.40	0.10	1.00		
Al_2O_3	−0.52	0.06	0.72	−0.06	−0.25	1.00	
Y_2O_3	−0.10	0.02	−0.28	0.12	−0.26	−0.20	1.00
Potůčky	**UO_2**	**PbO**	**SiO_2**	**P_2O_5**	**CaO**	**Al_2O_3**	**Y_2O_3**
UO_2	1.00						
PbO	0.35	1.00					
SiO_2	−0.78	−0.53	1.00				
P_2O_5	−0.87	−0.30	0.74	1.00			
CaO	0.75	0.41	−0.84	−0.74	1.00		
Al_2O_3	−0.68	−0.65	0.85	0.64	−0.69	1.00	
Y_2O_3	0.74	0.29	−0.67	−0.73	0.71	−0.66	1.00
Horní Slavkov	**UO_2**	**PbO**	**SiO_2**	**P_2O_5**	**CaO**	**Al_2O_3**	**Y_2O_3**
UO_2	1.00						
PbO	−0.48	1.00					
SiO_2	−0.66	0.07	1.00				
P_2O_5	−0.13	−0.22	0.37	1.00			
CaO	−0.35	0.72	−0.18	−0.23	1.00		
Al_2O_3	−0.83	0.62	0.70	0.02	0.38	1.00	
Y_2O_3	0.02	0.30	0.16	−0.02	0.27	0.23	1.00
Příbram	**UO_2**	**PbO**	**SiO_2**	**P_2O_5**	**CaO**	**Al_2O_3**	**Y_2O_3**
UO_2	1.00						
PbO	−0.38	1.00					
SiO_2	−0.48	−0.18	1.00				
P_2O_5	0.13	0.18	−0.14	1.00			
CaO	0.51	−0.08	−0.42	0.27	1.00		
Al_2O_3	−0.23	−0.29	0.60	−0.20	−0.23	1.00	
Y_2O_3	−0.22	0.04	0.21	0.12	−0.00	0.03	1.00
Zálesí	**UO_2**	**PbO**	**SiO_2**	**P_2O_5**	**CaO**	**Al_2O_3**	**Y_2O_3**
UO_2	1.00						
PbO	−0.43	1.00					
SiO_2	−0.30	−0.51	1.00				
P_2O_5	−0.50	−0.16	0.64	1.00			
CaO	−0.38	0.74	−0.38	−0.09	1.00		
Al_2O_3	0.34	−0.87	0.59	0.28	−0.73	1.00	
Y_2O_3	0.45	−0.73	0.26	0.07	−0.67	0.68	1.00

The concentrations of Y varied from below detection limit to 2.32 wt % Y_2O_3, which was found in uraninite from the Zálesí deposit. The elevated concentrations of Y were also found in uraninites from Jáchymov and Potůčky (about 1.2 wt % Y_2O_3). In uraninites from other vein-type uranium deposits, the Y concentrations were distinctly lower (0.02 wt %–0.59 wt % Y_2O_3) [43,45]. The highest to-date reported concentration of Y, as high as 0.79 wt % Y_2O_3, was found in uraninite from the Wittichen uranium deposit in the Black Forest ore district, SW Germany [13]. The highest reported concentrations of Y occurred in uraninites from high-temperature alkali-enriched magmatic rocks and pegmatites (up to 4.3 wt % Y_2O_3) [43]. At Potůčky, there was a strong positive correlation between

contents of Y and U (correlation coefficient = 0.74) coupled with strong negative correlations Y–Si (correlation coefficient −0.67) and Y–P (correlation coefficient −0.73; Table 4). These trends were the opposite to those observed for coffinite from Potůčky (Table 5), implying that the contents of Y are a primary feature of uraninite from Potůčky, which is not associated with superimposed coffinitization. In contrast, other studied sites did not display any statistically significant correlations between Y and U (Table 4).

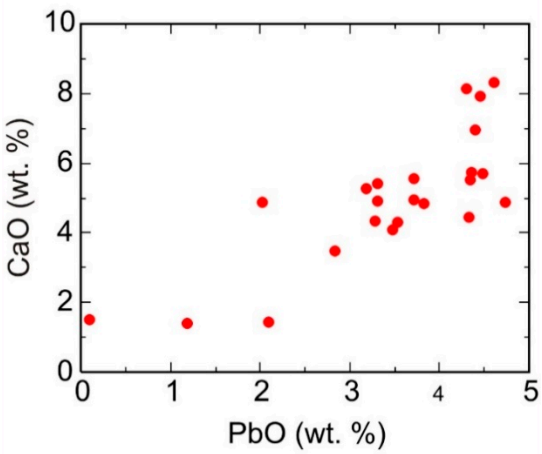

Figure 13. Distribution of Ca and Pb in uraninite from the Horní Slavkov uranium district.

5.2. Composition of Coffinite

Coffinite, nominally $USiO_4.nH_2O$ (n = 0–2) is an orthosilicate which may have a highly variable chemical composition. The tetravalent uranium can be partly substituted by U^{6+}, Ca^{2+}, Zr^{4+}, Th^{4+}, Y^{3+} and REE^{3+}, while atoms of silicon can be alternated with P^{5+}, As^{5+}, V^{5+}, S^{6+} and OH^- groups, including the possibility of vacancies in the tetrahedral site [40,49–51].

In the vein-type uranium deposits studied, coffinite often represented a younger uranium mineral arising from replacement of uraninite. Many of our microprobe analyses of coffinite, especially those from Zálesí, yielded SiO_2 concentrations too low to be assigned to the coffinite formula (U/Si > 1). Because in some cases SiO_2 and UO_2 contents varied continuously around compositions close to $USiO_4$ and UO_{2+x}, these transitional phases could be explained as mixtures of variable proportions of coffinite and uraninite [7,52] or possibly better by the gradual enrichment of Si in uraninite during its coffinitization. Similarly, gradual coffinitization of uraninite was described by Leroy and Holliger [45] from vein-type uranium deposits of the Massif Central in France. The wide variability in U/Si ratios of uraninite and coffinite and "patchy" textures of both minerals observed in the BSE images has been documented by Fojt et al. [9] at the Zálesí deposit. The authors interpreted these phenomena in terms of repeated coffinitization of uraninite and uraninitization of coffinite. The distinctly low totals of some of our microprobe analyses of coffinite (86.4 wt %–95.3 wt %) are probably due to the presence of water. In coffinite from Jáchymov the presence of H_2O was confirmed directly by infrared spectroscopy [7].

The concentration of Ca in the coffinites analyzed was lower than those in uraninites and varied from 0.6 wt % to 6.5 wt % CaO. Similar concentrations of Ca were also found in coffinite from vein-type uranium deposits in the Armorican Massif and Massif Central in France [45,53]. Positive correlations observed between the contents of Ca and U, together with negative correlations between Ca and Si contents in coffinites from Příbram and Horní Slavkov (Table 5) illustrates a greater affinity of Ca for uraninite than coffinite. At other sites, no such correlations occurred, perhaps due to superimposed alteration.

Lead is usually released from uraninite during coffinitization and does not enter the coffinite structure [7,45]. This is consistent with our data, showing lower concentrations of Pb in coffinite than

in uraninite. No statistically significant correlations occurred between contents of Pb and contents of U or Si in all coffinites studied (correlation coefficients $\leq$0.48; Table 5).

The concentrations of Th in our coffinites were low, from below detection limits to 0.21 wt % ThO_2. In coffinite from the Armorican Massif in France, the concentration of Th was below the detection limit of the electron microprobe [54]. Thorium-enriched coffinites were found in hydrothermal Fe–Cu–Au–Ag–U deposits at Olympic Dam (Australia), showing up to 3.61 wt % ThO_2 [53]. However, highly Th-enriched coffinite occurred in conglomerate-type uranium deposits from the Witwatersrand, South Africa, which contained up to 44.6 wt % ThO_2 [55].

The concentrations of Zr in our coffinites were usually below detection limits, but in some coffinite samples from the Jáchymov ore district, elevated contents of up to 3.3 wt % ZrO_2 were found. Elevated concentrations of Zr in coffinite from the Jáchymov deposit were also found by Janeczek (0.7 wt %–0.8 wt % ZrO_2) [7]. Zr-enriched coffinite occurred in some shear-zone hosted hydrothermal uranium deposits in the Bohemian Massif (Rožná, Okrouhlá Radouň) with contents of ZrO_2 up to 13.8 wt % [6].

Some coffinites from the vein-type uranium deposits studied were enriched in Y. In all cases, these uranium deposits contained superimposed five-element (Ag–Bi–As–Co–Ni) mineralization. The highest Y concentrations were found in coffinites from the Jáchymov uranium district (up to 5.5 wt % Y_2O_3) and the Zálesí deposit (up to 9.4 wt % Y_2O_3) (Figure 14). In both cases there was a positive correlation between Y and P (correlation coefficients 0.69 and 0.75, respectively; Table 5), and therefore the following substitution mechanisms could have been involved:

$$2U^{4+} = 2Y^{3+} + P^{5+} \text{ and/or } U^{4+} + Si^{4+} = Y^{3+} + P^{5+} \quad (1)$$

Y enriched coffinites containing up to 9.0 wt % Y_2O_3 were described from sandstone-hosted uranium deposits [56,57]. The coffinites from shear-zone hosted uranium deposits of the Bohemian Massif (Rožná, Okrouhlá Radouň) contained up to 3.4 wt % Y_2O_3 [6].

The P contents in coffinites analyzed varied from below detection limits to the elevated values recorded in coffinites from the Zálesí deposit (up to 4.1 wt % P_2O_5), Jáchymov district (up to 5.0 wt % P_2O_5) and the Potůčky deposit (up to 8.8 wt % P_2O_5). The P-rich coffinite from Potůčky occurred in association with Ca-U^{4+} phosphate ningyoite. P-enriched coffinite has been described from sandstone-related uranium deposits in the past, especially from Russia [56–60]. The highest content of P was found in coffinite from hydrothermal Fe–Cu–Au–Ag–U uranium deposits at Olympic Dam, Australia (up to 11.4 wt % P_2O_5) [53]. Other P-enriched coffinites occurred in a natural fission reactor at Bangombé, Gabon (up to 8.9 wt % P_2O_5) [58] and in the Khianga uranium district in the north-eastern Transbaikal region, Russia (up to 11 wt % P_2O_5) [60]. Enrichment of P in coffinites can be explained by substitution mechanisms coupled with Y and REE [53] and/or following substitution reactions, implying the existence of a solid solution between coffinite and ningyoite [57]:

$$U^{4+} + Si^{4+} = 2Ca^{2+} + 0.8P^{5+} + 0.2\square \quad (2)$$

$$U^{4+} + Si^{4+} = 2Ca^{2+} + P^{5+} + (OH)^{-} \quad (3)$$

With respect to the good correlation between P_2O_5 and Y_2O_3 contents in P-enriched coffinites from the Jáchymov district and Zálesí deposit (correlation coefficients 0.69 and 0.75, respectively; Table 5), the P enrichment in these coffinites can be explained by substitution reactions involving Y. By contrast, in P-rich coffinites from Potůčky there was a very good correlation between CaO and P_2O_5 (correlation coefficient 0.81; Table 5), which favours a solid solution between coffinite and ningyioite.

Table 5. Spearman correlation coefficients for selected elements analyzed in coffinite.

Jáchymov	**UO_2**	**PbO**	**SiO_2**	**P_2O_5**	**CaO**	**Al_2O_3**	**Y_2O_3**
UO_2	1.00						
PbO	0.01	1.00					
SiO_2	−0.33	−0.18	1.00				
P_2O_5	−0.61	−0.47	0.25	1.00			
CaO	−0.12	−0.26	−0.29	0.36	1.00		
Al_2O_3	0.08	0.34	0.37	−0.63	−0.44	1.00	
Y_2O_3	−0.72	−0.23	−0.01	0.69	0.09	−0.46	1.00
Potůčky	**UO_2**	**PbO**	**SiO_2**	**P_2O_5**	**CaO**	**Al_2O_3**	**Y_2O_3**
UO_2	1.00						
PbO	0.09	1.00					
SiO_2	−0.05	−0.31	1.00				
P_2O_5	−0.54	−0.15	0.06	1.00			
CaO	−0.23	−0.33	0.08	0.81	1.00		
Al_2O_3	0.16	−0.30	0.51	−0.23	−0.23	1.00	
Y_2O_3	−0.42	−0.04	−0.32	0.22	0.12	−0.54	1.00
Horní Slavkov	**UO_2**	**PbO**	**SiO_2**	**P_2O_5**	**CaO**	**Al_2O_3**	**Y_2O_3**
UO_2	1.00						
PbO	−0.04	1.00					
SiO_2	−0.80	−0.22	1.00				
P_2O_5	−0.64	−0.14	0.84	1.00			
CaO	0.74	−0.03	−0.73	−0.61	1.00		
Al_2O_3	−0.42	0.09	0.35	−0.08	−0.18	1.00	
Y_2O_3	0.10	−0.19	0.32	0.20	−0.32	0.00	1.00
Příbram	**UO_2**	**PbO**	**SiO_2**	**P_2O_5**	**CaO**	**Al_2O_3**	**Y_2O_3**
UO_2	1.00						
PbO	0.13	1.00					
SiO_2	−0.48	0.10	1.00				
P_2O_5	0.39	−0.30	−0.32	1.00			
CaO	0.54	0.16	−0.70	0.17	1.00		
Al_2O_3	−0.41	0.08	0.72	−0.55	−0.46	1.00	
Y_2O_3	−0.60	−0.03	0.49	−0.66	−0.48	0.63	1.00
Zálesí	**UO_2**	**PbO**	**SiO_2**	**P_2O_5**	**CaO**	**Al_2O_3**	**Y_2O_3**
UO_2	1.00						
PbO	0.02	1.00					
SiO_2	−0.45	−0.48	1.00				
P_2O_5	−0.73	−0.42	0.57	1.00			
CaO	−0.38	0.30	−0.17	0.16	1.00		
Al_2O_3	−0.11	−0.23	0.74	0.22	−0.06	1.00	
Y_2O_3	−0.40	−0.70	0.79	0.75	−0.06	0.57	1.00

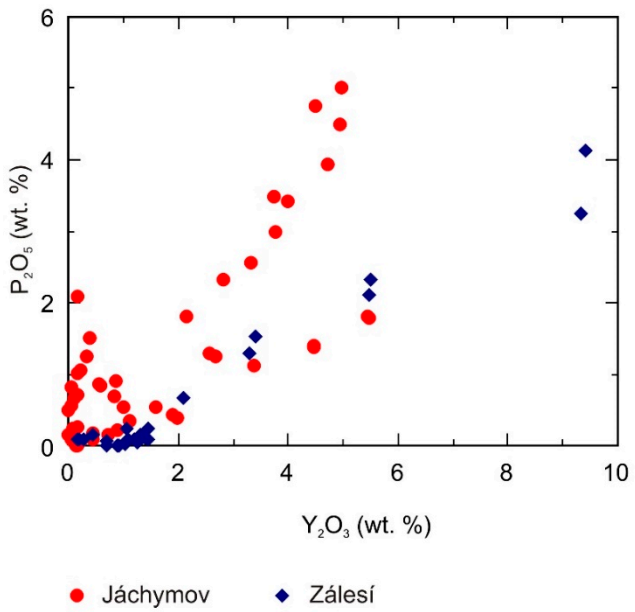

Figure 14. Distribution of P and Y in coffinite from the Jáchymov uranium district and the Zálesí uranium deposit.

5.3. Composition of Ningyoite

Ningyoite, nominally $(U,Ca,Ce)_2(PO_4)_2.1–2\ H_2O$, is a phosphate from the rhabdophane group with the general formula $AXO_4.1–2\ H_2O$, where A = Ca, REE, Th, U, Fe^{3+}, and X = P, S [61]. The presence of significant contents of P and Ca in the coffinite from Bangombé (Gabon) suggests a solid solution between coffinite and ningyoite [58]. In the Potůčky uranium deposit, ningyoite was found in close association with P-rich coffinite (Figure 12). The ningyoite was firstly established in the Ningyô-tôgé sandstone-type uranium deposit (Honshu Island, Japan) [62]. Later, ningyoite was also found in some other sandstone-type uranium deposits in Canada, Kazakhstan, Uzbekistan, Russia and Bulgaria [63–65]. In the Bohemian Massif, ningyoite occurred in the sandstone-type North Bohemian Cretaceous uranium district [61] and in some basement-hosted vein and shear-zone hydrothermal uranium deposits (Horní Slavkov, Jáchymov, Rožná) [10].

The chemical composition of ningyoite from the uranium deposits described above was thus far insufficiently described. Published works usually present chemical analyses containing only concentrations of U, P, Ca and Fe without determination of REE contents [10,61–63]. Ningyoite from the original locality in Japan contained 23.3 wt %–50.8 wt % UO_2, 6.1 wt %–11.5 wt % CaO, 4.8 wt % FeO, 16.8 wt %–29.4 wt % P_2O_5 and 5.4 wt %–9.3 wt % H_2O [62]. The composition of ningyoite from the North Bohemian uranium district was as follows: 42.5 wt %–49.9 wt % UO_2, 11.6 wt %–15.8 wt % CaO, 0.3 wt %–6.0 wt % FeO and 20.0 wt %–26.1 wt % P_2O_5 [61]. The composition of ningyoite from the Zdař Bůh ore cluster in the Horní Slavkov uranium district was: 26.3 wt %–41.7 wt % UO_2, 9.3 wt %–18.6 wt % CaO and 23.5 wt %–31.2 wt % P_2O_5 [10]. The chemical composition of ningyoite from the Potůčky uranium deposit (20.5 wt %–35.9 wt % UO_2, 7.5 wt %–9.4 wt % CaO, 20.3 wt %–26.1 wt % P_2O_5) is very similar to the composition of ningyoite from the original site in Japan. The chemical composition of ningyoite from uranium deposits in the former Soviet Union was never published, but according to Doynikova [66] the Ca/U ratio of ningyoites analyzed (ideally 1:1) varied from sample to sample, and generally Ca prevailed twice as often as U. The Ca/U ratio of ningyioite from Potůčky varied from 1.1 to 2.0 with a median value of 1.6.

The REE concentrations were only analyzed in ningyoite from the Ningyô-tôgé uranium deposit, where contents between 1.2 wt % and 3.8 wt % REE_2O_3 and only moderate LREE/HREE fractionation (La_N/Yb_N = 0.6–8.6) were found [67]. The total REE concentrations in ningyoite from Potůčky were

distinctly higher (13.5 wt %–22.3 wt % REE_2O_3) with significant enrichment in middle REE and a similar La_N/Yb_N ratio (0.8–11.7) (Figure 15).

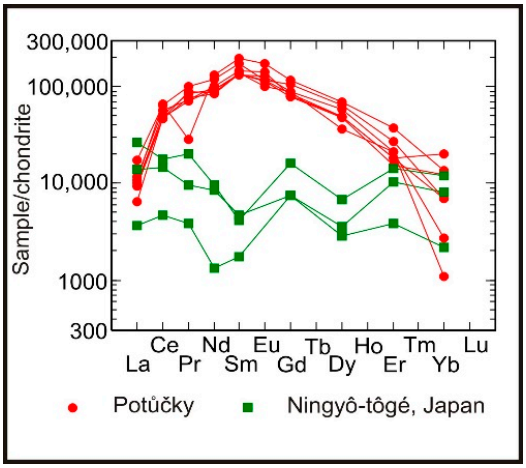

Figure 15. Chondrite-normalised rare earth element patterns for ningyoite from the Potůčky and Ningyô-tôgé uranium deposits. Chondrite values are from Anders and Grevesse [68], data for Ningyô-tôgé deposit are from Muto [67].

6. Conclusions

Uraninite, coffinite and ningyoite mineralization from hydrothermal veins of the Příbram, Jáchymov, Horní Slavkov ore districts and the Potůčky, Zálesí and Předbořice uranium deposits have been studied in this paper. These Late Variscan deposits are situated in low-grade to high-grade metamorphic rocks and/or folded sedimentary rocks of the basement of the Bohemian Massif. Uraninite always represented the primary uranium phase at these localities, whereas coffinite and ningyoite originated mostly during superimposed alteration of primary uraninite. The uraninites analyzed contained variable concentrations of Pb (mostly 1.5 wt %–5.4 wt %, locally up to 10.8 wt % PbO), Ca (0.7 wt %–8.3 wt % CaO), and Si (up to 10.0 wt % SiO_2). The contents of Th, Zr, REE and Y were low, mainly below the detection limits of the electron microprobe. The highest concentration of Th was found in uraninite from the Horní Slavkov ore district (up to 0.2 wt % ThO_2), the highest concentration of Zr (up to 0.7 wt % ZrO_2) contained uraninite from the Jáchymov ore district and the highest concentration of Y was found in uraninite from the Zálesí uranium deposit (up to 2.3 wt % Y_2O_3).

Coffinite from the vein-type deposits studied usually emerged through gradual coffinitization of uraninite. The concentrations of CaO were lower than those in uraninites and varied from 0.6 to 6.5 wt %. Coffinite from the Jáchymov ore district was partly enriched in Zr (up to 3.3 wt % ZrO_2). Coffinites from uranium deposits containing superimposed "five-element" (Ag–Bi–As–Co–Ni) mineralization were enriched in Y (up to 2.5 wt %, 5.5 wt % and 9.4 wt % Y_2O_3 for Potůčky, Jáchymov and Zálesí deposits, respectively). Coffinite from the Potůčky uranium deposit was distinctly enriched in P (up to 8.8 wt % P_2O_5) and occurred in association with the very rare ningyoite.

Ningyoite was found together with P-rich coffinite in veinlets cutting altered uraninite in samples from Potůčky. The composition of ningyoite was similar to that of the type locality in Japan; however, ningyoite from the Potůčky uranium deposit was distinctly enriched in REE (up to 22.3 wt % REE_2O_3).

Supplementary Materials: The following are available online at http://www.mdpi.com/2075-163X/9/2/123/s1, Table S1: Electron microprobe analyses of selected elements in all uraninites analyzed, Table S2: Electron microprobe analyses of selected elements in all coffinites analyzed, Table S3: Electron microprobe analyses of selected elements in all ningyoites analyzed.

Author Contributions: M.R. wrote a significant part of paper, Z.D. analyzed all samples on the electron microprobe, J.S. contributed some samples from the Jáchymov uranium district, P.S. contributed some samples

from the Příbram uranium district and V.Š. contributed some samples from the Jáchymov uranium district and all samples from the Potůčky uranium deposit.

Funding: This research was funded by Czech Science Foundation, grant number [19–05360S] and by Ministry of Culture, Czech Republic, grant number [DKRVO 2018/02].

Acknowledgments: The research for this paper was carried out thanks to the support of the long-term conceptual development research organisation of IRSM AS CR (RVO 67985891) and projects of the National Museum (DKRVO 2019-2023/1.II.a, 00023272). We are grateful to two anonymous reviewers for numerous comments and recommendations that helped to improve this paper. We wish also to thank Annika Szameitat and John Brooker for their English corrections.

Conflicts of Interest: The authors declare no conflict of interest.

References

1. Arapov, J.A.; Boitsov, V.J.; Česnokov, N.I.; Diakonov, A.V.; Halbrštát, J.; Jakovjenko, A.M.; Kolek, M.; Komínek, J.; Kozyrev, V.N.; Kremtschukov, G.A.; et al. *Czechoslovak Uranium Deposits*; ČSUP: Příbram, Czechoslovakia, 1984; pp. 1–368. (In Czech)
2. Kafka, J. *Czech Ore and Uranium Mining Industry*; Anagram: Ostrava, Czech Republic, 2003; pp. 1–647. (In Czech)
3. René, M. Uranium hydrothermal deposits. In *Uranium: Characteristics, Occurrence and Human Exposure*, 1st ed.; Vasiliev, A.Y., Sidorov, M., Eds.; Nova Science Publishers, Inc.: New York, NY, USA, 2012; pp. 211–244.
4. Kříbek, B.; Žák, K.; Dobeš, P.; Leichmann, J.; Pudilová, M.; René, M.; Scharm, B.; Scharmová, M.; Hájek, A.; Holeczy, D.; et al. The Rožná uranium deposit (Bohemian Massif, Czech Republic): Shear zone-hosted, late Variscan and post-Variscan hydrothermal mineralization. *Miner. Deposita* **2009**, *44*, 99–128. [CrossRef]
5. René, M. Alteration of granitoids and crystalline rocks and uranium mineralisation in the Bor pluton area, Bohemian Massif, Czech Republic. *Ore Geol. Rev.* **2017**, *81*, 188–200. [CrossRef]
6. René, M.; Dolníček, Z. Uraninite, coffinite and brannerite from shear-zone hosted uranium deposits of the Bohemian Massif (Central European Variscan belt). *Minerals* **2017**, *7*, 50. [CrossRef]
7. Janeczek, J. Composition and origin of coffinite from Jáchymov, Czechoslovakia. *N. Jb. Miner. Mh.* **1991**, *9*, 385–395.
8. Ondruš, P.; Veselovský, F.; Gabašová, A.; Hloušek, J.; Šrein, V.; Vavřín, I.; Skála, R.; Sejkora, J.; Drábek, M. Primary minerals of the Jáchymov ore district. *J. Czech. Geol. Soc.* **2003**, *48*, 19–155.
9. Fojt, B.; Dolníček, Z.; Kopa, D.; Sulovský, P.; Škoda, R. Paragenesis of the hypogene associations from the uranium deposit at Zálesí near Javorník in Rychlebské hory Mts., Czech Republic. *Čas. Slez. Muz. Opava* **2005**, *A54*, 223–280. (In Czech)
10. Dymkov, Y.M.; Boitsov, V.M.; Preobrazhensky, A.N.; Ivanova, O.A. Ningyoite from hydrothermal veins of the Gorni Slavkov (CSSR). *Mineral. Zh.* **1986**, *8*, 34–43. (In Russian)
11. Budinger, P.A.; Drenski, T.L.; Varnes, A.W.; Mooney, J.R. The case of the Great Yellow Cake Caper. *Anal. Chem.* **1980**, *52*, 942A–948A. [CrossRef]
12. Mercadier, J.; Cuney, M.; Lach, P.; Boiron, M.-C.; Bonhoure, J.; Richard, A.; Leisen, M.; Kister, P. Origin of uranium deposits revealed by their rare earth element signature. *Terra Nova* **2011**, *23*, 264–269. [CrossRef]
13. Frimmel, H.E.; Schedel, S.; Brätz, H. Uraninite chemistry as forensic tool for provenance analysis. *Appl. Geochem.* **2014**, *48*, 104–121. [CrossRef]
14. Mayer, K.; Wallenius, M.; Lützenkirchen, K.; Horta, J.; Rasmussen, G.; van Belle, P.; Varga, Z.; Buda, R.; Erdmann, N.; Kratz, J.V.; et al. Uranium from German nuclear projects of the 1940s—A nuclear forensis investigation. *Angew. Chem. Int. Ed. Engl.* **2015**, *54*, 13452–13456. [CrossRef] [PubMed]
15. Kristo, M.J.; Gaffney, A.M.; Marks, N.; Knight, K.; Cassata, W.S.; Hutcheon, I.D. Nuclear Forensis Science: Analysis of nuclear material out of regulatory control. *Ann. Rev. Earth Planet. Sci.* **2016**, *44*, 555–579. [CrossRef]
16. Spano, T.L.; Simonetti, A.; Balboni, E.; Dorais, C.; Burns, P.C. Trace element and U isotope analysis of uraninite and ore concentrate: Applications for nuclear forensic investigations. *Appl. Geochem.* **2017**, *84*, 277–285. [CrossRef]
17. Kříbek, B.; Žák, K.; Spangenberg, J.; Jehlička, J.; Prokeš, S.; Komínek, J. Bitumens in the Late Variscan hydrothermal vein-type uranium deposit of Příbram, Czech Republic: Sources, radiation-induced alteration, and relation to mineralization. *Econ. Geol.* **1999**, *94*, 1093–1114. [CrossRef]

18. Holub, F.; Machart, J.; Manová, M. The Central Bohemian plutonic complex: Geology, chemical composition and genetic interpretation. *Sbor. Geol. Věd. LG* **1997**, *31*, 27–50.
19. Janout, T.; Škubal, M. The north-south trending dislocations and the end of the clay fault in the Příbram area. *Věst. Ústř. Úst. Geol.* **1968**, *43*, 441–448.
20. Škácha, P.; Goliáš, V.; Sejkora, J.; Plášil, J.; Strnad, L.; Škoda, R.; Ježek, J. Hydrothermal uranium-base metal mineralization of the Jánská vein, Březové Hory, Příbram, Czech Republic: Lead isotopes and chemical dating of uraninite. *J. Geosci.* **2009**, *54*, 1–13. [CrossRef]
21. Petroš, R.; Prokeš, S.; Komínek, J. Uranium deposit of Příbram, Czechoslovakia. In *Vein Type Uranium Deposits, IAEA-TECDOC 361*; International Atomic Energy Agency: Vienna, Austria, 1986; pp. 307–317.
22. Anderson, E.B. *Isotopic-Geochronological Investigation of Uranium Deposits of Czechoslovakia*; Unpublished report Czechoslovak Uranium Industry 1862-87; Czechoslovak Uranium Industry: Příbram, Czechoslovakia, 1987; pp. 1–32. (In Russian)
23. Kroner, U.; Hahn, T.; Romer, R.L.; Linnemann, U. The Variscan orogeny in the Saxo-Turingian zone—Heterogeneous overprint of Cadomian/Paleozoic Peri-Gondwana crust. *Geol. Soc. Amer. Spec. Pap.* **2007**, *423*, 153–172.
24. Komínek, J.; Chrt, J.; Landa, O. Uranium mineralization in the western Krušné hory Mts. (Erzgebirge) and the Slavkovský les region, Czech Republic. In *Monograph Series on Mineral Deposits*; 31; Gebrüder Borntraeger: Berlin, Germany; Stuttgart, Germany, 1994; pp. 209–230.
25. Legierski, J. Model ages and isotopic composition of ore leads of the Bohemian Massif. *Čas. Mineral. Geol.* **1973**, *18*, 1–23.
26. Förster, B.; Haack, U. U/Pb Datierungen von Pechblenden und die hydrothermale Entwicklung der U-Lagerstätte Aue-Niederschlema (Erzgebirge). *Z. Geol. Wiss.* **1996**, *23*, 581–588.
27. Pluskal, O. The post war history of Czechoslovak uranium from Jáchymov (Joachimsthal). *Czech Geol. Survey, Spec. Pap.* **1998**, *9*, 1–48. (In Czech)
28. Runge, W. *Chronicle of Bismut*; CDROM. Wismut GmbH: Chemnitz, Germany, 1999; pp. 1–2738. (In German)
29. Sejkora, J.; Šrein, V.; Šreinová, B.; Dolníček, Z. Selenide mineralization of the uranium deposit Potůčky, Krušné hory mountains (Czech Republic). *Bull. Mineral. Petrolog.* **2017**, *25*, 306–317.
30. Borkowska, M.; Choukroune, P.; Hameuret, J.; Martineau, F. A geochemical investigation of the age, significance and structural evolution of the Caledonian-Variscan granite-gneisses of the Snieznik metamorphic area (Central Sudetes, Poland). *Geol. Sudetica* **1990**, *25*, 1–27.
31. Turniak, K.; Mazur, S.; Wysoczański, R. SHRIMP zircon geochronology and geochemistry of the Orlica-Śnieżnik gneisses (Variscan belt of Central Europe) and their tectonic implications. *Geodinam. Acta* **2000**, *13*, 293–312. [CrossRef]
32. Dolníček, Z.; Fojt, B.; Prochaska, W.; Kučera, J.; Sulovský, P. Origin of the Zálesí U–Ni–Co–As–Ag/Bi deposit, Bohemian Massif, Czech Republic: Fluid inclusion and stable isotope constraints. *Miner. Deposita* **2009**, *44*, 81–97. [CrossRef]
33. Borkowska, M.; Dörr, W. Some remarks on the age and mineral chemistry of orthogneisses from the Ladek-Snieznik metamorphic massif–Sudetes, Poland. *Terra Nostra* **1998**, *2*, 27–30.
34. Šuráň, J.; Veselý, T. Small uranium deposits in the crystalline complexes of the Bohemian Massif. Part IV: The region of Eastern Bohemia and Moravia. *Geol. Hydrometalurg. Uranu* **1982**, *6*, 3–50. (In Czech)
35. Blüml, A.; Tacl, A.; Rus, V. The occurrence of selenium minerals in southwest part of the Sedlčany-Krásná Hora metamorphosed island. *Čas. Miner. Geol.* **1964**, *9*, 73. (In Czech)
36. Blüml, A.; Tacl, A.; Rus, V. Selenides from the southwestern tract of the Sedlčany-Krásná Hora islet. *Čas. Miner. Geol.* **1966**, *11*, 37–45. (In Czech)
37. Johan, Z. Merenskyite, $Pd(Te,Se)_2$, and the low-temperature selenide association from the Předbořice uranium deposit, Czechoslovakia. *N. Jb. Min. Mh.* **1989**, *4*, 179–191.
38. Bindi, L.; Förster, H.-J.; Grundmann, G.; Keutsch, F.N.; Stanley, C.J. Petříčekite, $CuSe_2$, a new member of the marcasite group from the Předbořice deposit, Central Bohemia region, Czech Republic. *Minerals* **2016**, *6*, 33. [CrossRef]
39. Pouchou, J.J.; Pichoir, F. "PAP" (ϕ-ρ-Z) procedure for improved quantitative microanalysis. In *Microbeam Analysis*; Armstrong, J.T., Ed.; San Francisco Press: San Francisco, CA, USA, 1985; pp. 104–106.
40. Janeczek, J.; Ewing, R.C. Structural formula of uraninite. *J. Nucl. Mater.* **1992**, *190*, 128–132. [CrossRef]

41. Janeczek, J.; Ewing, R.C. Dissolution and alteration of uraninite under reducing conditions. *J. Nucl. Mater.* **1992**, *190*, 157–173. [CrossRef]
42. Cathelineau, M.; Cuney, M.; Leroy, J.; Lhote, F.; Nguyen Trung, C.; Pagel, M.; Poty, B. Mineralogical characteristics of the pitchblendes in the Hercynian province of Europe. Comparison with the uranium oxides of Proterozoic age occurring in various deposits in North America, Africa and Australia. In *Vein-Type and Similar Uranium Deposits in Rocks Younger than Proterozoic. Proc. Tech. Comm. Meet. Lisabon, 24–28 September 1979*; International Atomic Energy Agency: Vienna, Austria, 1982; pp. 159–177. (In French)
43. Alexandre, P.; Kyser, K.; Layton-Matthews, D.; Joy, B. Chemical compositions of natural uraninite. *Can. Mineral.* **2016**, *53*, 1–30. [CrossRef]
44. Golubev, V.N.; Cuney, M.; Poty, B. The phase composition and U-Pb-isotopic systems of pitchblende of quartz-calcite-pitchblende veins of the Schlema-Alberoda deposit (Erzgebirge Mts.). *Geol. Rud. Mestorozd.* **2000**, *42*, 513–525. (In Russian)
45. Leroy, J.; Holliger, P. Mineralogical, chemical and isotopic (U–Pb method) studies of Hercynian uraniferous mineralizations (Margnac and Fanay mines, Limousin, France). *Chem. Geol.* **1984**, *45*, 121–134. [CrossRef]
46. Shahin, H.A.A. Geochemical characteristics and chemical electron microprobe U-Pb-Th dating of pitchblende mineralization from Gabal Gattar Younger granite, North Eastern Desert, Egypt. *Open J. Geol.* **2014**, *4*, 24–32. [CrossRef]
47. Zhao, D.; Ewing, R.C. Alteration products of uraninite from the Colorado Plateau. *Radiochim. Acta* **2000**, *88*, 739–750. [CrossRef]
48. Havelcová, M.; Machovič, V.; Mizera, J.; Sýkorová, I.; René, M.; Borecká, L.; Lapčák, L.; Bičáková, O.; Janeček, O.; Dvořák, Z. Structural changes in amber due to uranium mineralization. *J. Environ. Radioactiv.* **2016**, *158–159*, 89–101. [CrossRef] [PubMed]
49. Stieff, L.R.; Stern, T.W.; Sherwood, A.M. Coffinite, a uranous silicate with hydroxyl substitution—A new mineral. *Am. Mineral.* **1956**, *41*, 675–688.
50. Finch, R.J.; Hanchar, J.M. Structure and chemistry of zircon and zircon group minerals. In *Zircon. Reviews in Mineralogy and Geochemistry*; Hanchar, J.M., Hoskin, P.W.O., Eds.; Mineralogical Society of America and the Geochemical Society: Chantilly, VA, USA, 2003; Volume 53, pp. 1–26.
51. Deditius, A.P.; Utsonomiya, S.; Wall, M.A.; Pointeau, V.; Ewing, R.C. Crystal chemistry and radiation-induced amorphization of P-coffinite from the natural fission reactor at Bangombé, Gabon. *Am. Mineral.* **2009**, *94*, 827–836. [CrossRef]
52. Frenzel, G.; Otteman, J. On a new Ni-As mineral and a remarkable uranium mineralization from the Anna Procopi mine near Příbram. *N. Jb. Min. Mh.* **1968**, *11*, 420–429. (In German)
53. Macmillan, E. The Evolution of Uraninite, Coffinite and Brannerite from the Olympic Dam Iron Oxide-Copper-Gold-Silver-Uranium Deposit: Linking Textural Observations to Compositional Variability. Master's Thesis, University of Adelaide, Adelaide, Australia, 2016.
54. Cathelineau, M. Les gisements d´uranium lies spatialement aux leucogranites Sudarmoricains et à leur encaissant métamorphique. Relations et interactions entre les minéralisations et divers contexts géologiques et structuraux. *Sci. Terre Mem.* **1982**, *42*, 1–375.
55. Smits, G. (U, Th)-bearing silicates in reefs of the Witwatersrand, South Africa. *Can. Mineral.* **1989**, *27*, 643–655.
56. Hansley, P.L.; Fitzpatrick, J.J. Compositional and crystallographic data on REE-bearing coffinite from the Grants uranium region, northwestern New Mexico. *Am. Mineral.* **1989**, *74*, 263–270.
57. Doynikova, O.A.; Sidorenko, G.A. The mineralogy of tetravalent uranium. *New Data Miner.* **2010**, *45*, 79–90.
58. Janeczek, J.; Ewing, R. Phosphatian coffinite with rare earth elements and Ce-rich françoisite-(Nd) from sandstone beneath a natural fission reactor at Bangombé, Gabon. *Mineral. Mag.* **1996**, *60*, 665–669. [CrossRef]
59. Doynikova, O.A.; Sidorenko, G.A.; Sivtsov, A.V. Phosphosilicates of tetravalent uranium. *Dokl. Earth Sci.* **2014**, *456*, 755–758. [CrossRef]
60. Doynikova, O.A.; Tarasov, N.N.; Mokhov, A.V. A new phosphatic type of uranium deposits in Russia. *Dokl. Earth Sci.* **2014**, *457*, 910–914. [CrossRef]
61. Scharmová, M.; Scharm, B. Rabdophane group minerals in the uranium ore district of northern Bohemia (Czech Republic). *J. Czech Geol. Soc.* **1994**, *39*, 267–280.
62. Muto, T.; Meyrowitz, R.; Pommer, A.M.; Murano, T. Ningyoite, a new uranous phosphate mineral from Japan. *Am. Mineral.* **1959**, *44*, 633–650.

63. Boyle, D.R.; Littlejohn, A.L.; Roberts, A.C.; Watson, D.M. Ningyoite in uranium deposits of south-central British Columbia: First North America occurrence. *Can. Mineral.* **1981**, *19*, 325–331.
64. Doynikova, O.A. Uranium deposits with a new phosphate type of blacks. *Geol. Ore Deposits* **2007**, *49*, 89–96. [CrossRef]
65. Popov, K.; Velichkov, D.; Popov, P. The post-collisional Upper Thracian Rift System (Bulgaria) and the formed exogenous uranium deposits. Part 2—Metallogeny of the Upper Thracian uranium ore region. *Rev. Bulgar. Geol. Soc.* **2016**, *77*, 51–64.
66. Doynikova, O.A. Genetic crystal chemistry of the mineral components of uranium blacks. *Geochem. Int.* **2003**, *12*, 1325–1331.
67. Muto, T. The precipitation environment of ningyoite. *Miner. J.* **1962**, *3*, 306–337. [CrossRef]
68. Anders, E.; Grevesse, N. Abundances of the elements: Meteoritic and solar. *Geochim. Cosmochim. Acta* **1989**, *53*, 197–214. [CrossRef]